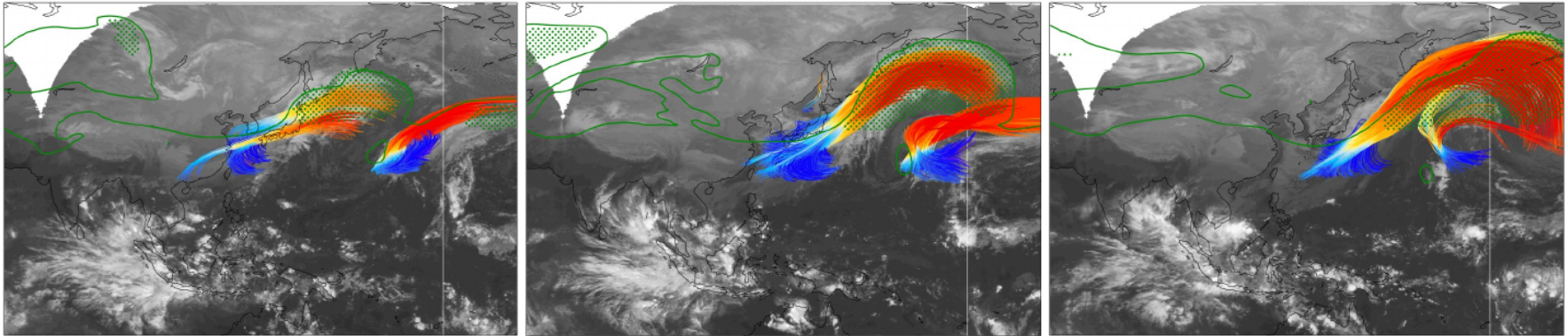


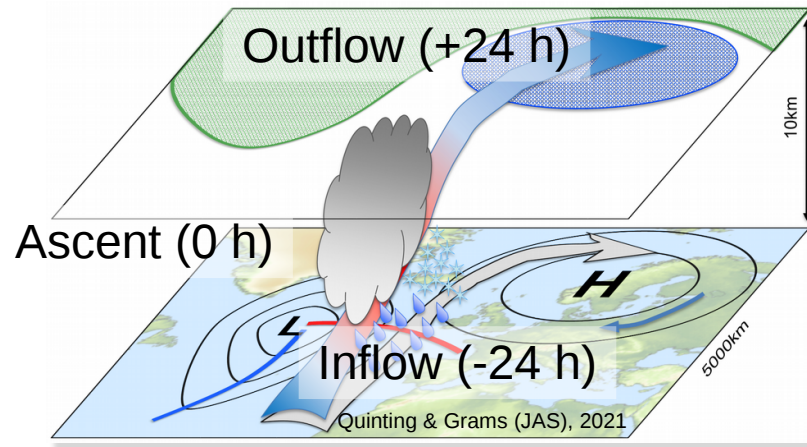
Importance of the representation of warm conveyor belts for the predictability of the large-scale flow on sub-seasonal time scales

Julian Quinting, Karlsruhe Institute of Technology

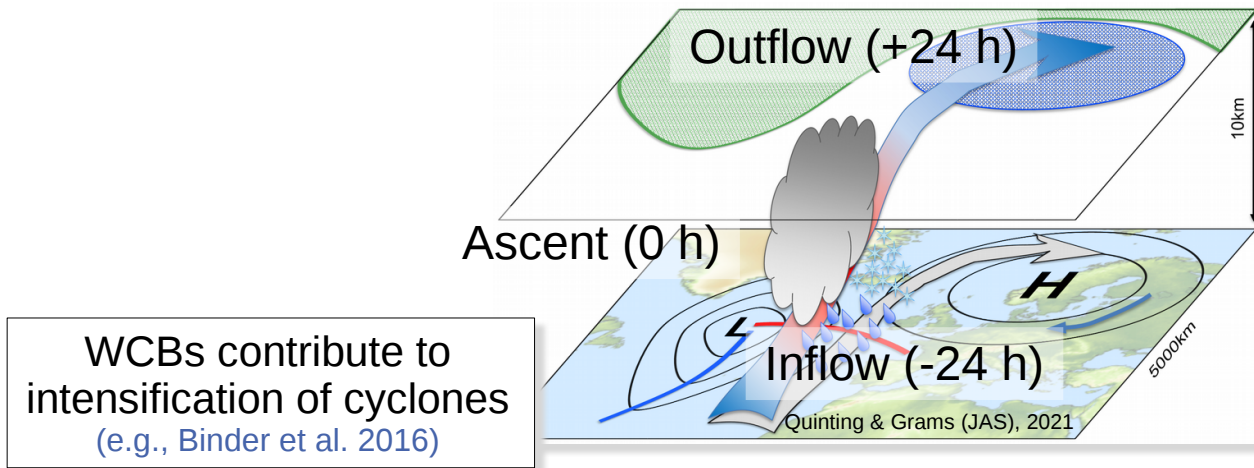
with contributions from Christian M. Grams, Jan Wandel, Peter Knippertz, Stephan Pfahl, and Heini Wernli



Role of WCBs for large-scale dynamics and predictability



Role of WCBs for large-scale dynamics and predictability

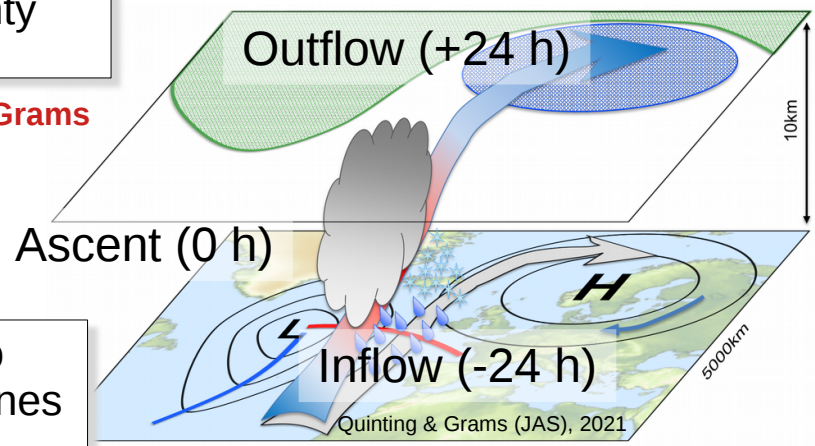


Role of WCBs for large-scale dynamics and predictability

WCBs are source/magnifier
of forecast uncertainty
(e.g., Grams et al. 2018)

see Poster presented by C. Grams
in poster session 2

WCBs contribute to
intensification of cyclones
(e.g., Binder et al. 2016)

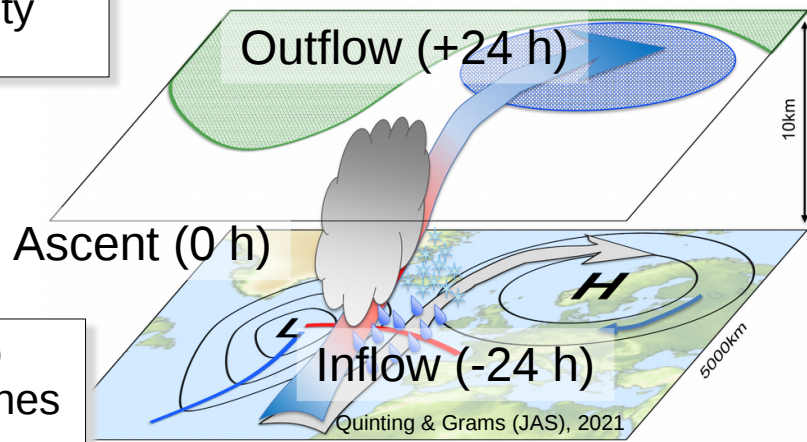


Role of WCBs for large-scale dynamics and predictability

WCBs are source/magnifier
of forecast uncertainty
(e.g., Grams et al. 2018)

WCBs affect lifecycle of
blocking anticyclones
(e.g., Steinfeld & Pfahl 2019)

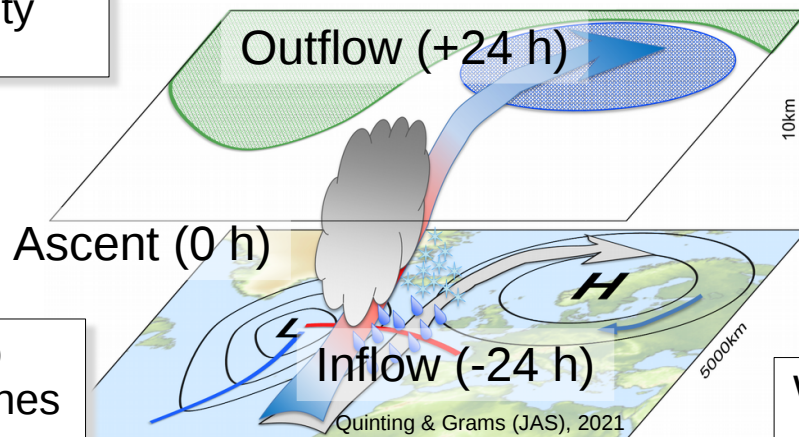
WCBs contribute to
intensification of cyclones
(e.g., Binder et al. 2016)



Role of WCBs for large-scale dynamics and predictability

WCBs are source/magnifier of forecast uncertainty
(e.g., Grams et al. 2018)

WCBs contribute to intensification of cyclones
(e.g., Binder et al. 2016)



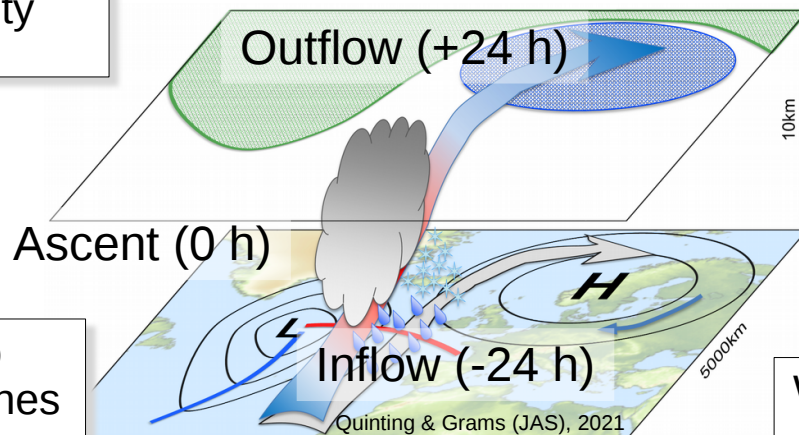
WCBs affect lifecycle of blocking anticyclones
(e.g., Steinfeld & Pfahl 2019)

WCBs are associated with precipitation extremes
(e.g., Pfahl et al. 2014)

Role of WCBs for large-scale dynamics and predictability

WCBs are source/magnifier of forecast uncertainty
(e.g., Grams et al. 2018)

WCBs affect lifecycle of blocking anticyclones
(e.g., Steinfeld & Pfahl 2019)



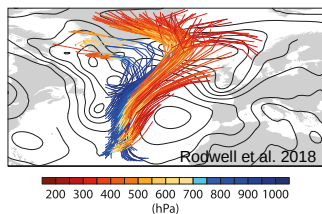
WCBs contribute to intensification of cyclones
(e.g., Binder et al. 2016)

WCBs are associated with precipitation extremes
(e.g., Pfahl et al. 2014)

Accurate representation of WCBs in weather and climate models desirable

An Eulerian WCB Metric (ELIAS 2.0)

Data	ERA-INTERIM (<i>Dee et al. 2010</i>)
amount	~ 58,400 time steps
availability	Grid: 1° at 61 vertical model levels Temporal availability: 6-hourly

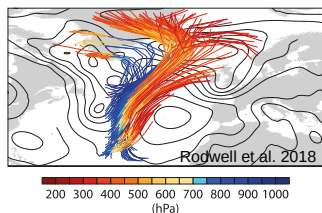


Trajectory calculation



An Eulerian WCB Metric (ELIAS 2.0)

Data	ERA-INTERIM <i>(Dee et al. 2010)</i>	S2S ensemble reforecasts
amount	~ 58,400 time steps	~ 10^6 to 10^7 time steps
availability	Grid: 1° at 61 vertical model levels Temporal availability: 6-hourly	Grid: 1.5° at 10 pressure levels Temporal availability: 24-hourly



Trajectory calculation

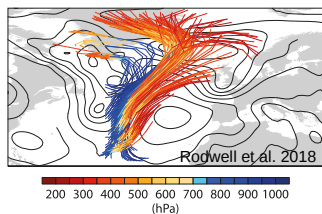


Trajectory calculation



An Eulerian WCB Metric (ELIAS 2.0)

Data	ERA-INTERIM <i>(Dee et al. 2010)</i>	S2S ensemble reforecasts
amount	~ 58,400 time steps	~ 10^6 to 10^7 time steps
availability	Grid: 1° at 61 vertical model levels Temporal availability: 6-hourly	Grid: 1.5° at 10 pressure levels Temporal availability: 24-hourly



Trajectory calculation



Trajectory calculation



**Eulerian metric to identify signature of WCB stages
based on Unet-type convolutional neural network**

An Eulerian WCB Metric (ELIAS 2.0)

Predictor selection

- Predictors based on standard input fields at pressure levels: T , q_v , Z , u , v

P	WCB inflow	WCB ascent	WCB outflow
1	700-hPa thickness advection	850-hPa relative vorticity	300-hPa relative humidity
2	850-hPa meridional moisture flux	700-hPa relative humidity	300-hPa irrotational wind speed
3	1000-hPa moisture flux convergence	300-hPa thickness advection	500-hPa static stability
4	500-hPa moist potential vorticity	500-hPa meridional moisture flux	300-hPa relative vorticity
5	conditional probability of ascent (+24 h)*	30-d WCB ascent climatology**	conditional probability of ascent (-24 h)*

Quinting and Grams (2021), JAS

[doi:10.1175/JAS-D-20-0139.1](https://doi.org/10.1175/JAS-D-20-0139.1)

An Eulerian WCB Metric (ELIAS 2.0)

Predictor selection

- Predictors based on standard input fields at pressure levels: T, q_v , Z, u, v

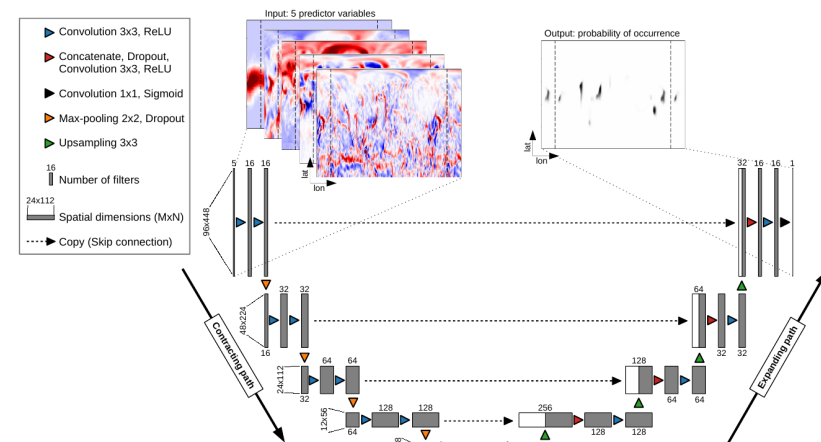
P	WCB inflow	WCB ascent	WCB outflow
1	700-hPa thickness advection	850-hPa relative vorticity	300-hPa relative humidity
2	850-hPa meridional moisture flux	700-hPa relative humidity	300-hPa irrotational wind speed
3	1000-hPa moisture flux convergence	300-hPa thickness advection	500-hPa static stability
4	500-hPa moist potential vorticity	500-hPa meridional moisture flux	300-hPa relative vorticity
5	conditional probability of ascent (+24 h)*	30-d WCB ascent climatology**	conditional probability of ascent (-24 h)*

Quinting and Grams (2021), JAS

[doi:10.1175/JAS-D-20-0139.1](https://doi.org/10.1175/JAS-D-20-0139.1)

Unet-type convolutional neural network

- Trained on global ERA-Interim at 1° grid spacing



Quinting and Grams (2022), [doi:10.5194/gmd-15-715-2022](https://doi.org/10.5194/gmd-15-715-2022)

https://git.scc.kit.edu/nk2448/wcbmetric_v2

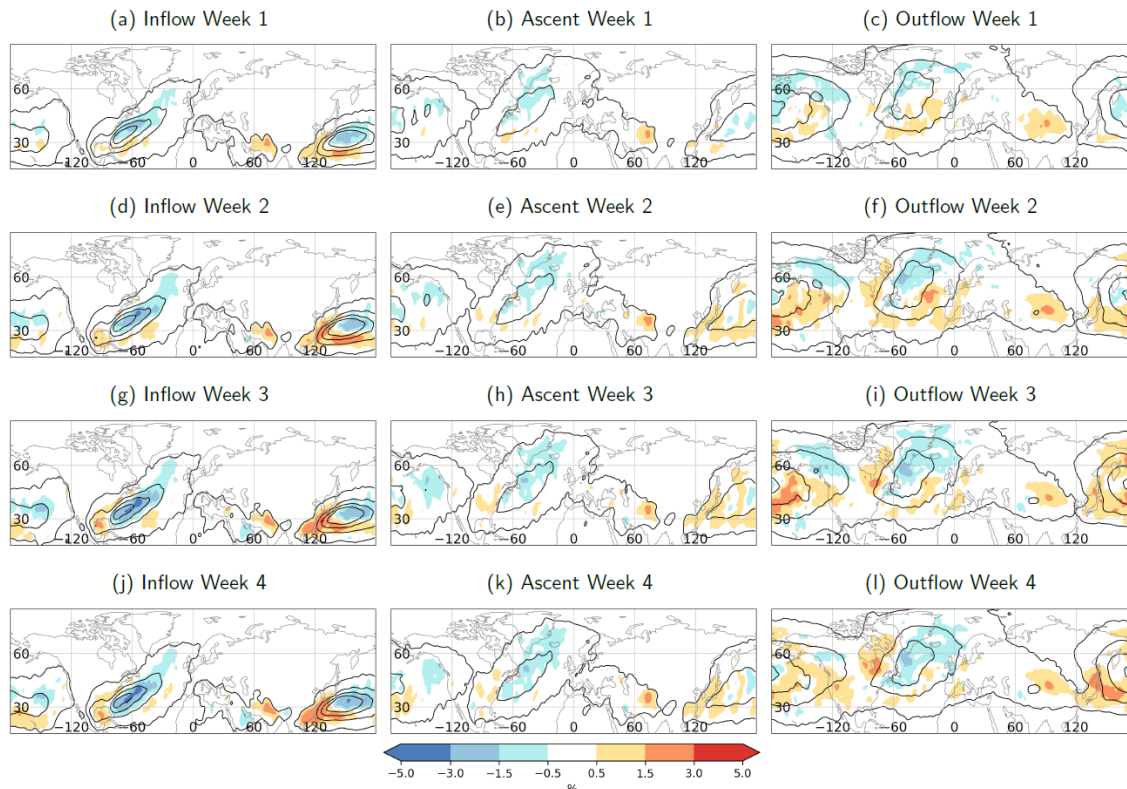
WCB frequency biases in S2S IFS reforecasts (PhD Jan Wandel)

WCB biases 1997-2017 (DJF)
(CY43R1, CY43R3, CY43R5)

Systematic **underestimation**
of **WCB activity** in northern
North Atlantic

WCB frequency biases
saturate in **week 2**

WCB outflow biases coincide
with biases in geopotential



DJF WCB climatology at 1, 5, 10, 15%

Wandel et al. 2021, JAS, doi: [10.1175/JAS-D-20-0385.1](https://doi.org/10.1175/JAS-D-20-0385.1)
here shown for ELIAS 2.0 PhD Dissertation Jan Wandel (2022)

WCB outflow skill in S2S IFS reforecasts (PhD Jan Wandel)

WCB skill 1997-2017 (DJF)
(CY43R1, CY43R3, CY43R5)

Daily forecast skill horizon
limited to about 7-9 days

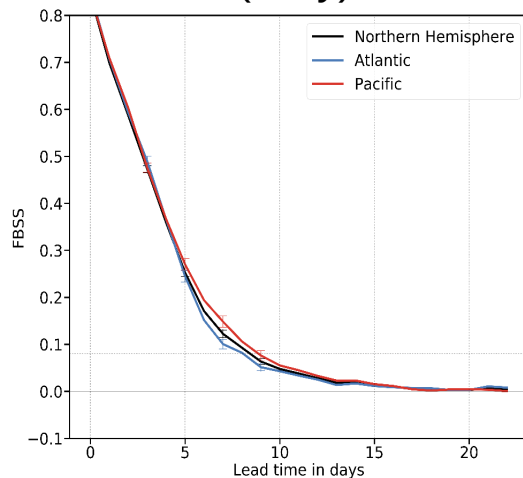
Skill up to week 2 for weekly
mean

Skill over North Pacific higher
than over North Atlantic

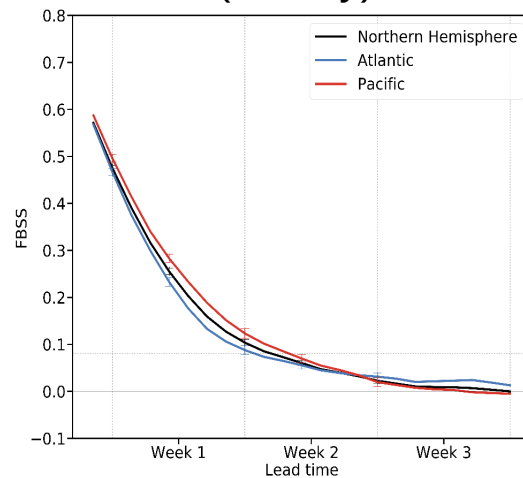


**Influence of modes of tropical
convection (e.g., MJO)?**

WCB outflow skill
(daily)

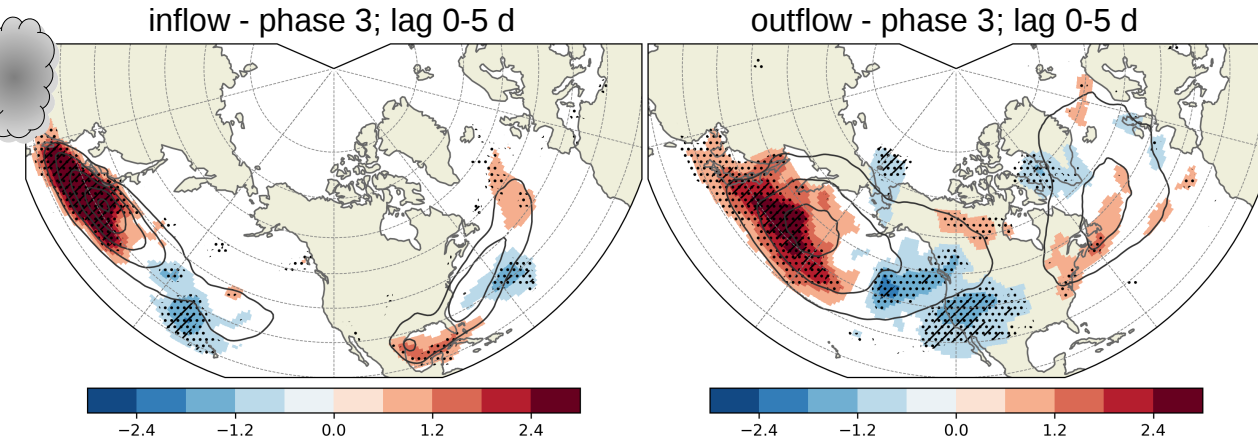


WCB outflow skill
(weekly)

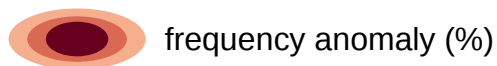
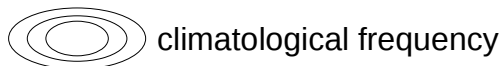


Wandel et al. 2021, JAS, doi: [10.1175/JAS-D-20-0385.1](https://doi.org/10.1175/JAS-D-20-0385.1)
here shown for ELIAS 2.0 PhD Dissertation Jan Wandel (2022)

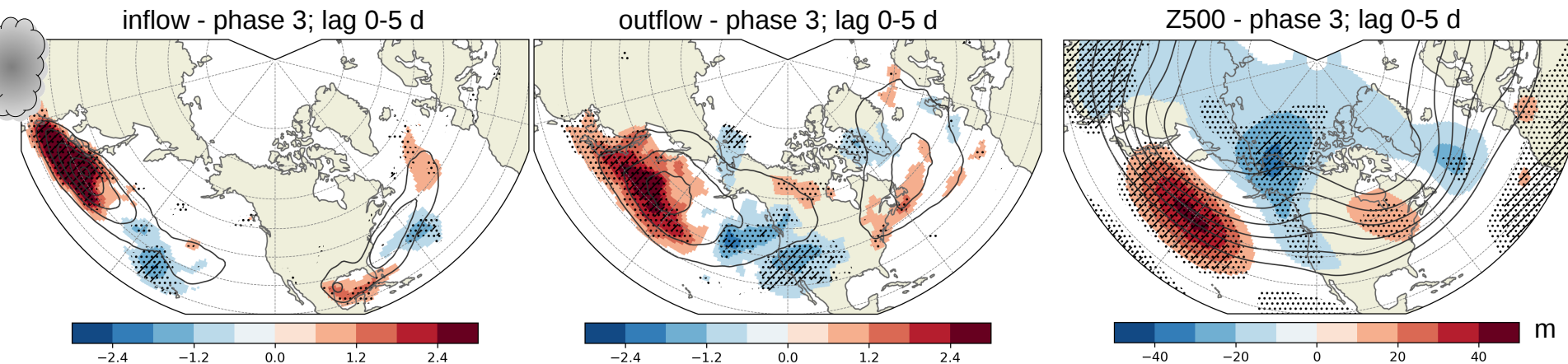
MJO modulates WCB activity



WCB activity increases significantly over the western North Pacific during/after MJO phase 3 (cf. [Guo et al. 2017](#))



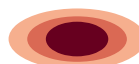
MJO modulates WCB activity



WCB activity increases significantly over the western North Pacific during/after MJO phase 3 (cf. Guo et al. 2017)

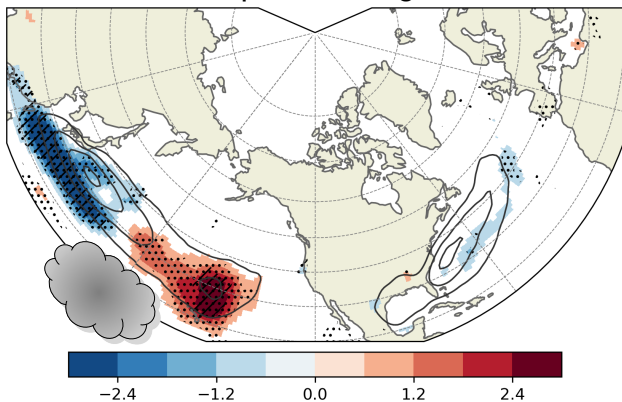
Anomalous ridging over Pacific (e.g., Moore et al. 2010)

 climatological frequency

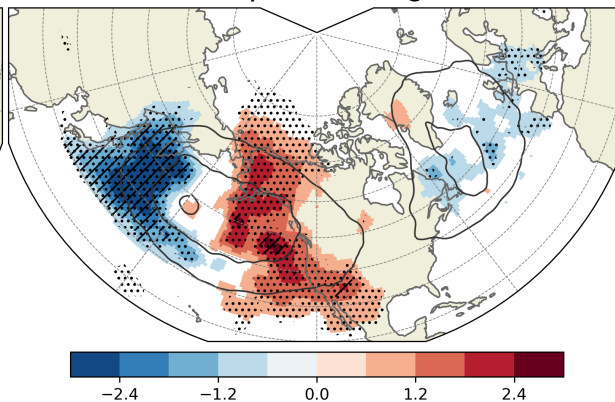
 frequency anomaly (%)

MJO modulates WCB activity

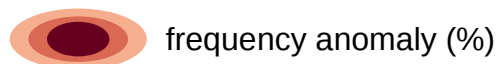
inflow - phase 7; lag 0-5 d



outflow - phase 7; lag 0-5 d

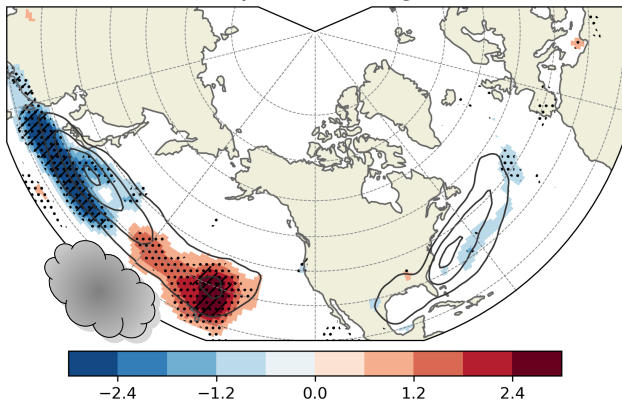


WCB activity increases significantly over the eastern North Pacific during/after MJO phase 7

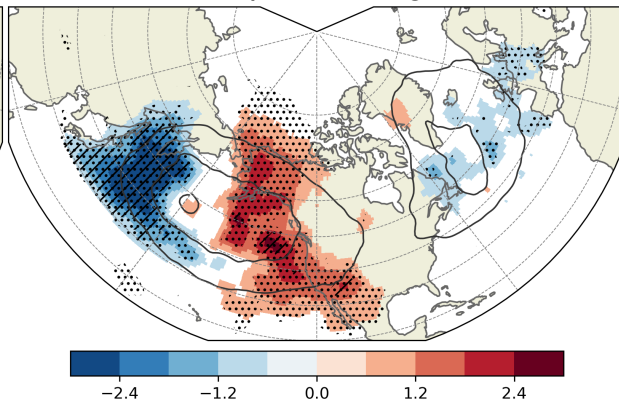


MJO modulates WCB activity

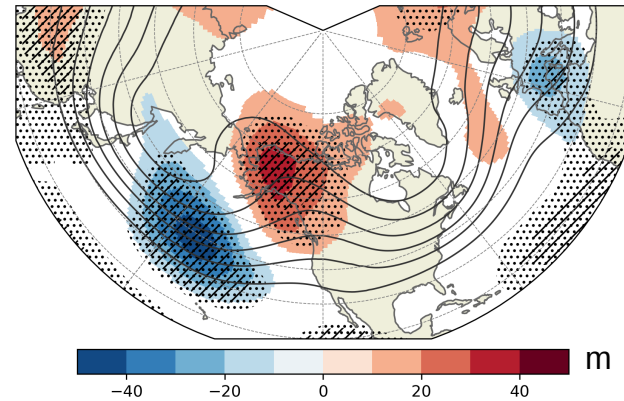
inflow - phase 7; lag 0-5 d



outflow - phase 7; lag 0-5 d

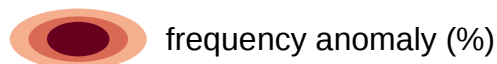


Z500 - phase 7; lag 0-5 d

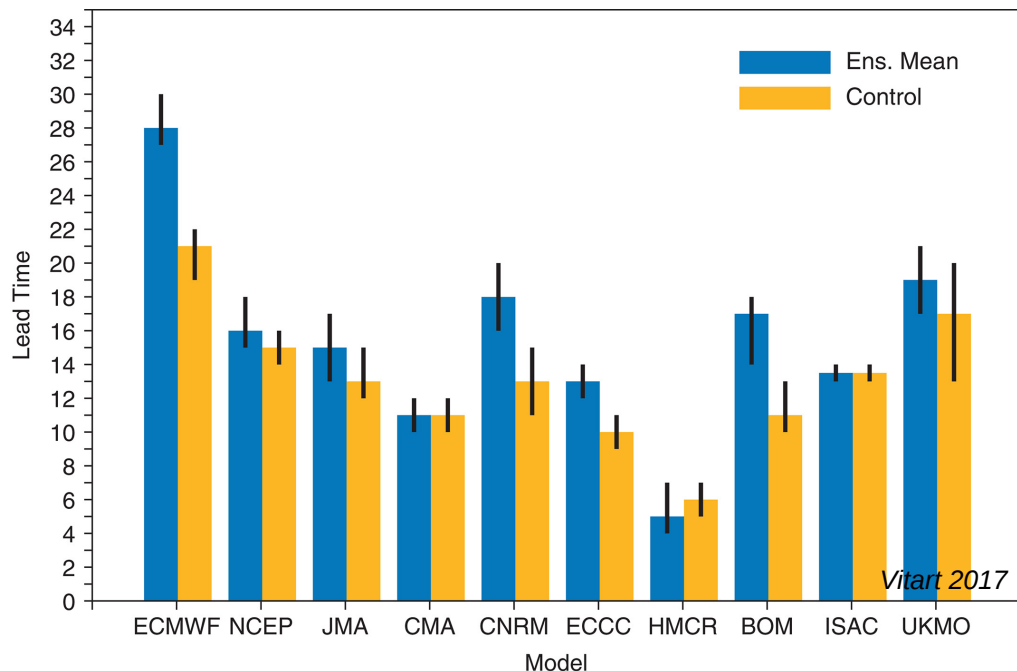


WCB activity increases significantly over the eastern North Pacific during/after MJO phase 7

Anomalous ridging over Alaska (e.g., [Henderson et al. 2016](#))



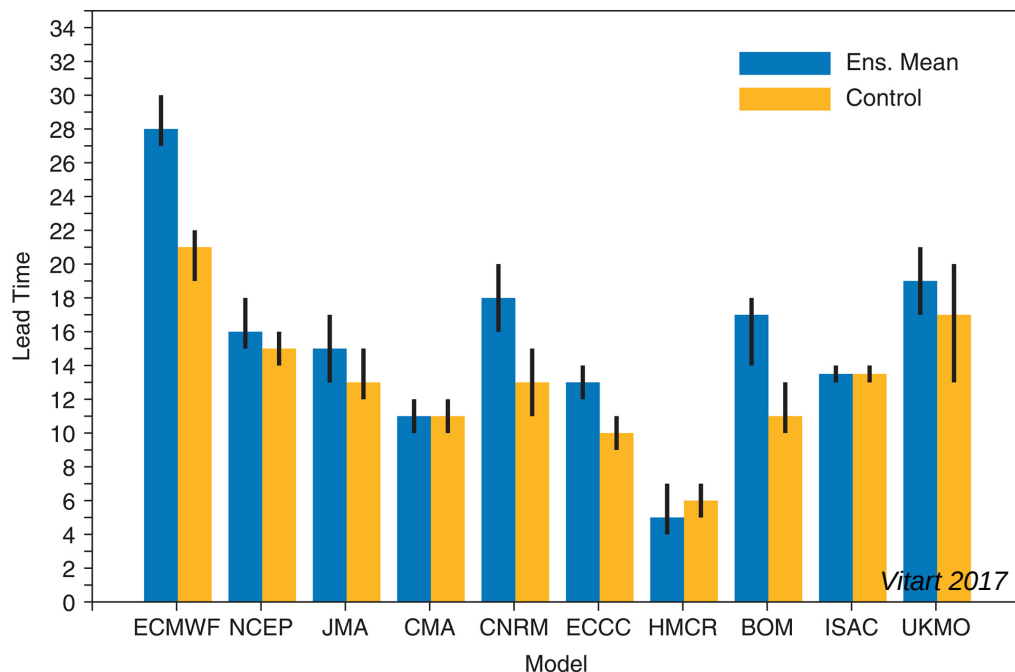
How is this modulation represented in S2S IFS reforecasts?



Current NWP models skillfully predict
the MJO out to 28 days

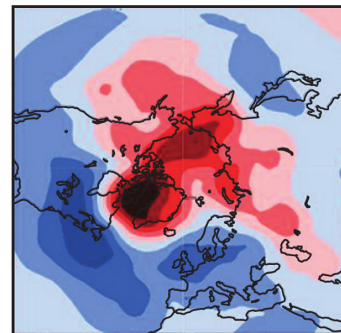
(Vitart 2017)

How is this modulation represented in S2S IFS reforecasts?



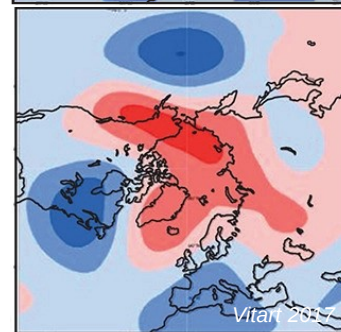
Current NWP models skillfully predict the MJO out to 28 days

(Vitart 2017)



ERA-Interim

Z500 anomaly 11-15 days after phase 7



S2S IFS reforecast

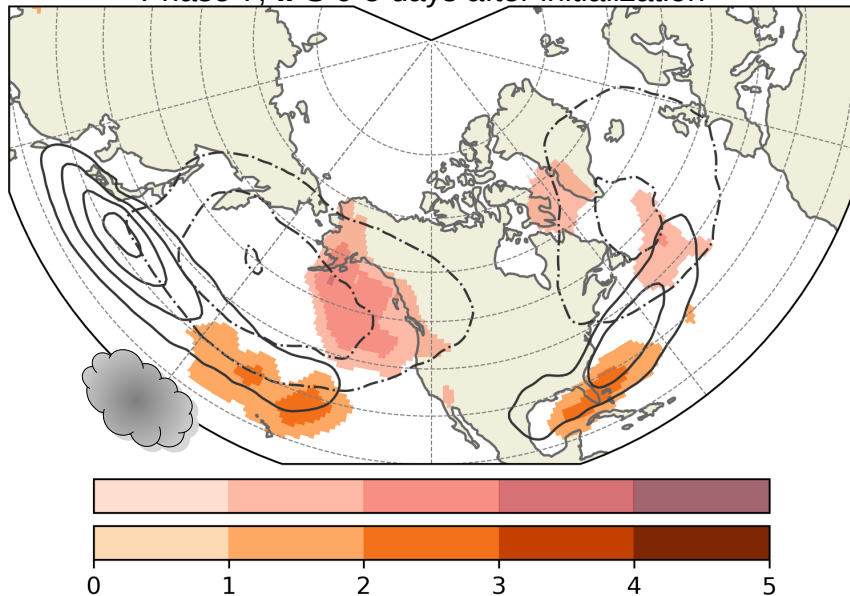
Z500 anomaly 11-15 days after phase 7

Teleconnection signals are weakening with forecast lead time

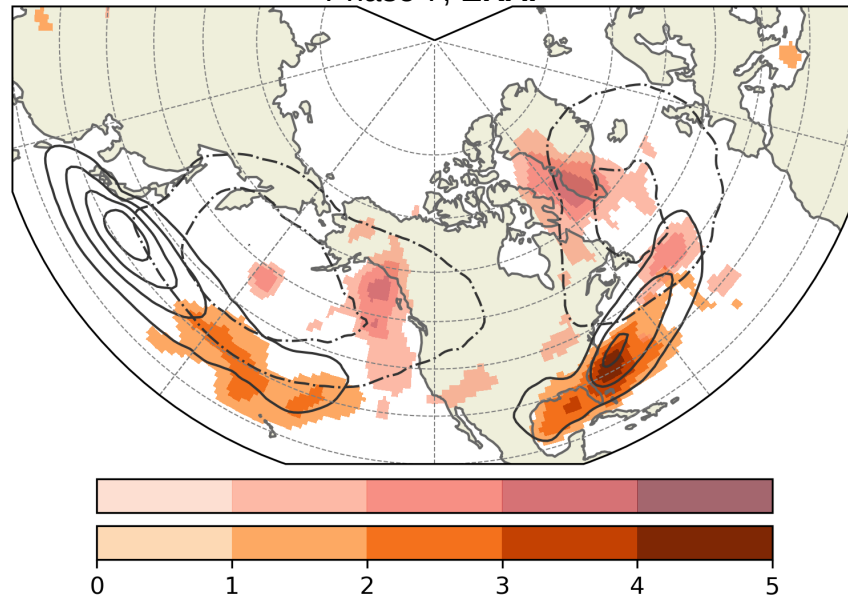
(Vitart 2017)

How is this modulation represented in S2S IFS reforecasts?


Phase 7; IFS 0-5 days after initialization



Phase 7; ERAI



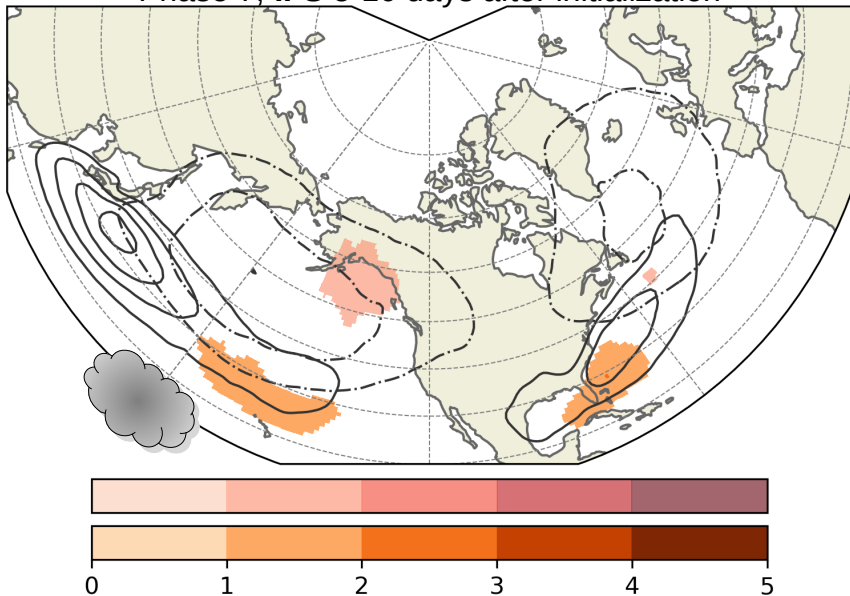
At early leadtimes ECMWF's S2S forecast represent WCB increase over eastern Pacific after phase 7.

 pos. inflow frequency anomaly

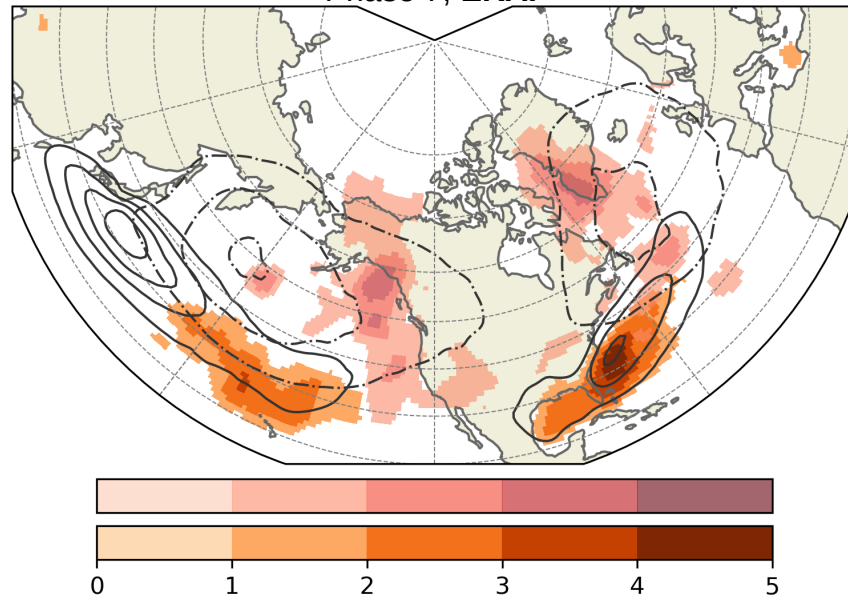
 pos. outflow frequency anomaly

How is this modulation represented in S2S IFS reforecasts?


Phase 7; IFS 5-10 days after initialization



Phase 7; ERAI



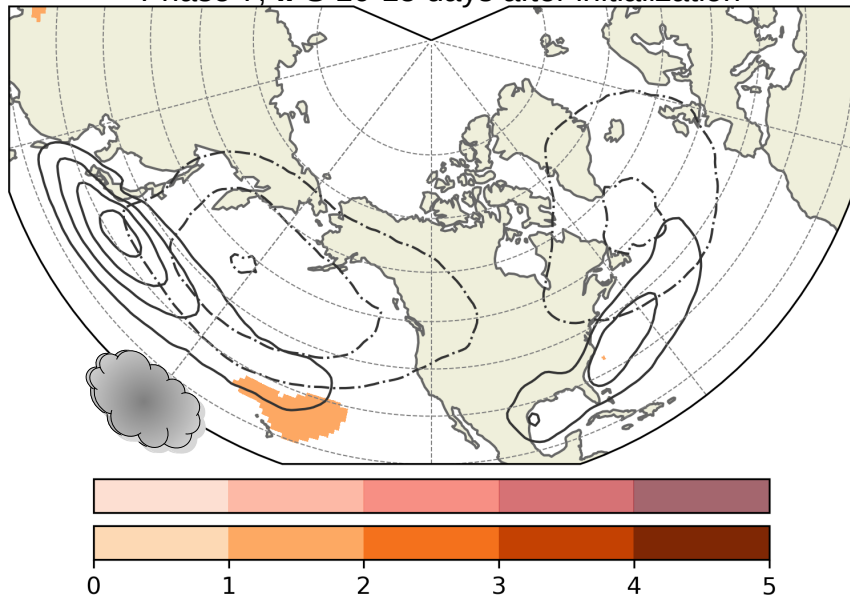
Anomalous WCB activity ceases in reforecasts
after 5-10 days forecast lead time

 pos. inflow frequency anomaly

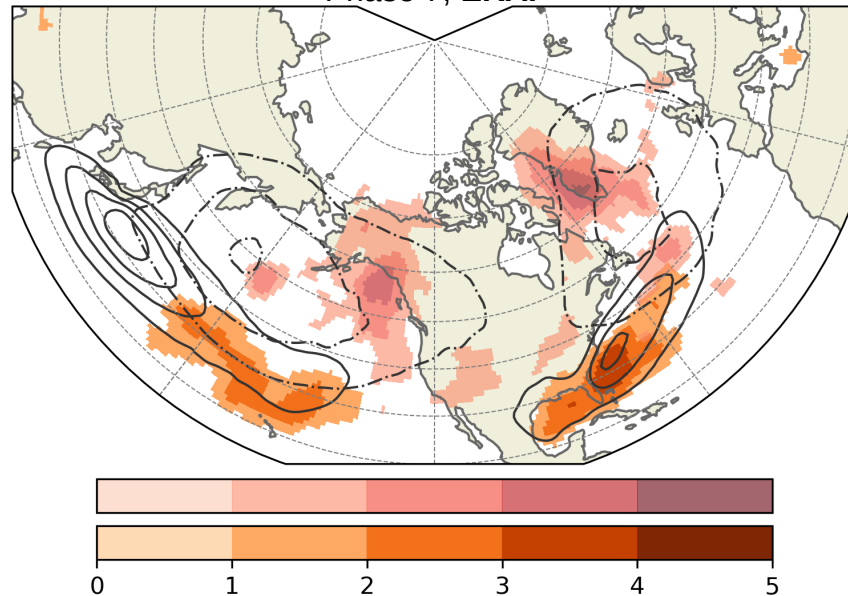
 pos. outflow frequency anomaly

How is this modulation represented in S2S IFS reforecasts?


Phase 7; IFS 10-15 days after initialization



Phase 7; ERAI



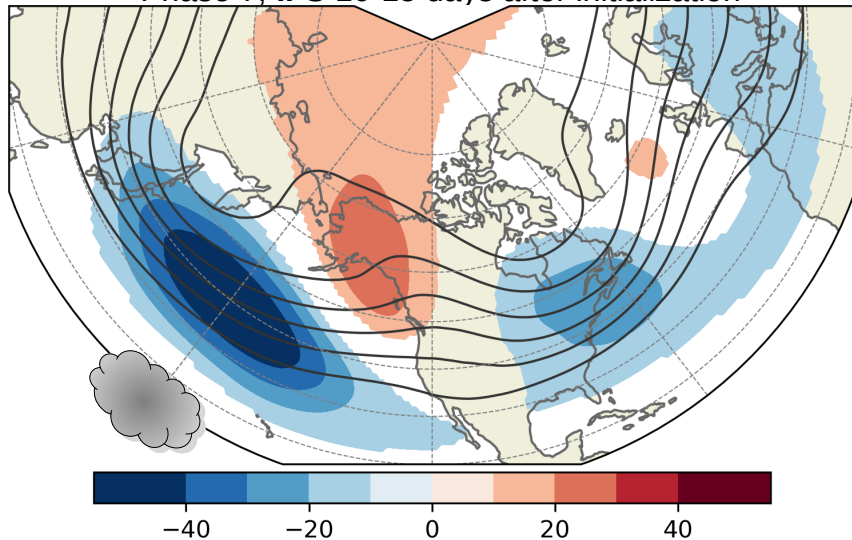
Anomalous WCB activity ceases in reforecasts
after 5-10 days forecast lead time

 pos. inflow frequency anomaly

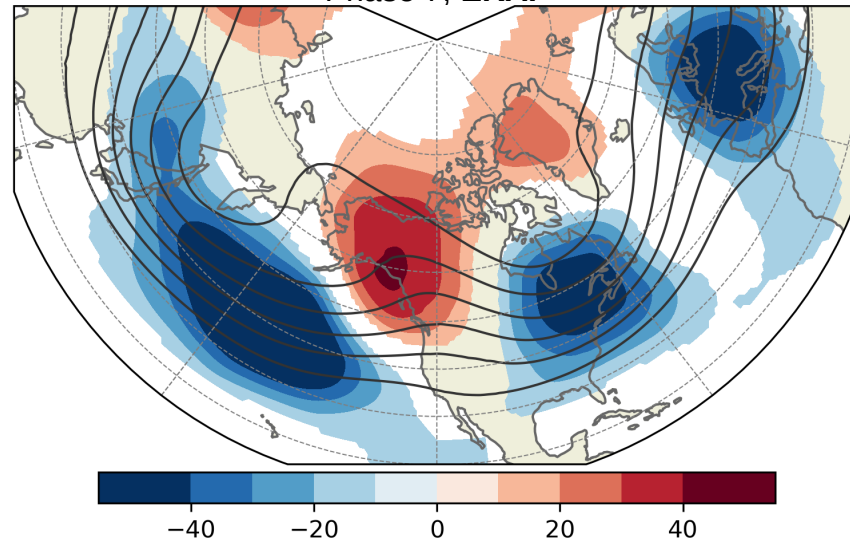
 pos. outflow frequency anomaly

How is this modulation represented in S2S IFS reforecasts?

Phase 7; IFS 10-15 days after initialization



Phase 7; ERAI



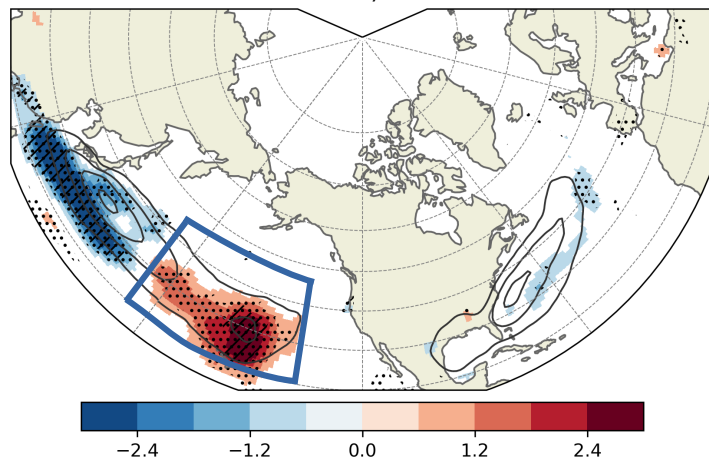
Anomalous outflow frequency and ridge over western North America are underestimated. Coincidence or causality?

 500-hPa geopotential height anomaly

Implications for MJO phase 7 with unusually high WCB activity

Consider all forecasts that were initialized 5 days before observed phase 7 with pentad of abnormally high/low WCB activity

Phase 7; ERAI



climatological frequency

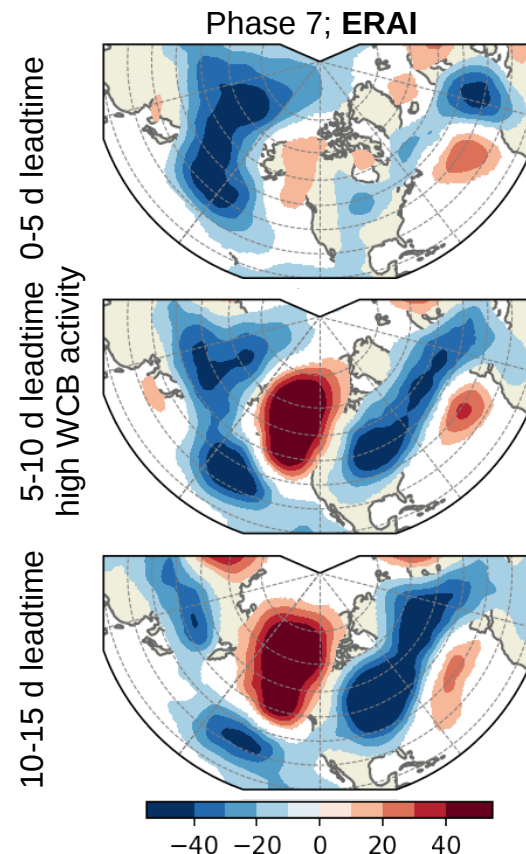


Inflow frequency anomaly (%)

Implications for MJO phase 7 with unusually high WCB activity

High amplitude ridge/blocking develops over western North America

Canonical teleconnection pattern towards NAO- does not establish

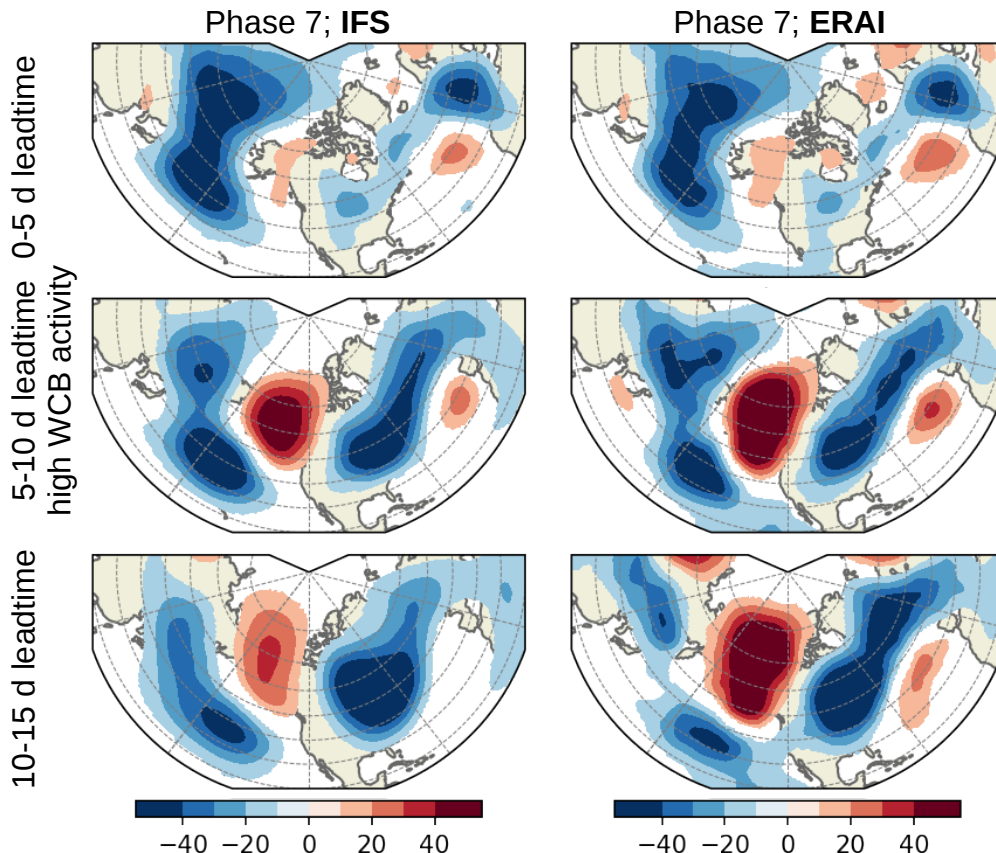


Implications for MJO phase 7 with unusually high WCB activity

High amplitude ridge/blocking develops over western North America

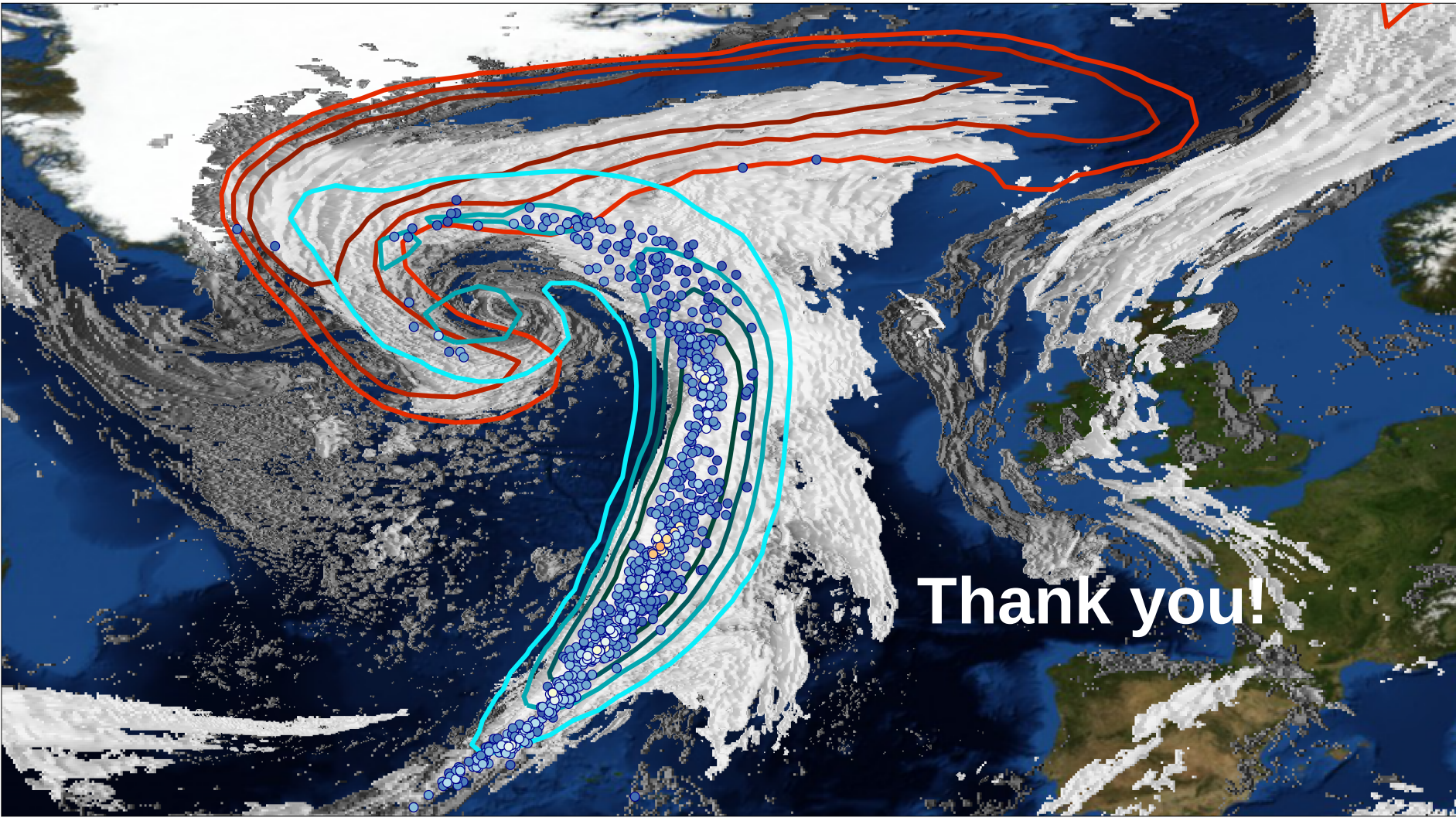
Canonical teleconnection pattern towards NAO- does not establish

High amplitude ridge in IFS S2S reforecasts weakens more rapidly than in ERAI



Take-home messages

- Deep learning models skillfully identify footprints of Lagrangian airstreams at **significantly reduced costs** and from data at coarse resolution
- systematic biases in WCB occurrence in S2S reforecasts affect Rossby wave pattern
- weekly **WCB skill up to 2 weeks**
- WCB activity is modulated by MJO
→ in line with studies on ECs and ARs (Moore et al. 2010; Mundhenk et al. 2016; Guo et al. 2017)
- modulation of **WCB activity weakens beyond 10 days** lead time
- underestimation of ridge building over western North America after phase 7 correlates with too low WCB outflow activity
→ cause of a long-standing problem in extended-range forecasts? (e.g., Vitart 2017)



Thank you!

Model documentation

Description of model development and evaluation:

<https://doi.org/10.5194/gmd-2021-276>
Preprint. Discussion started: 22 September 2021
© Author(s) 2021. CC BY 4.0 License.



Geoscientific
Model Development
Discussions



EuLerian Identification of ascending Air Streams (ELIAS 2.0) in Numerical Weather Prediction and Climate Models. Part I: Development of deep learning model

Application examples:

<https://doi.org/10.5194/gmd-2021-278>
Preprint. Discussion started: 28 September 2021
© Author(s) 2021. CC BY 4.0 License.



Geoscientific
Model Development
Discussions



EuLerian Identification of Ascending air Streams (ELIAS 2.0) in Numerical Weather Prediction and Climate Models. Part II: Model application to different data sets



*Trained-models and
example scripts
available on [Gitlab!](#)*